PROCEEDINGS OF SCIENCE

The static energy of a quark-antiquark pair from Laplacian eigenmodes

Roman Höllwieser,[a,*] **Francesco Knechtli**[a] **and Mike Peardon**[b]

[a] *Dept. of Physics, Bergische Universität Wuppertal,*
Gaußstrasse 20, 42119 Wuppertal, Germany
[b] *School of Mathematics, Trinity College,*
Dublin 2, Ireland
E-mail: hoellwieser@uni-wuppertal.de, knechtli@uni-wuppertal.de, mjp@maths.tcd.ie

We test a method for computing the static quark-antiquark potential in lattice QCD, which is not based on Wilson loops, but where the trial states are formed by eigenvector components of the covariant lattice Laplace operator. The runtime of this method is significantly smaller than the standard Wilson loop calculation, when computing the static potential not only for on-axis, but also for many off-axis quark-antiquark separations, *i.e.*, when a fine spatial resolution is required. We further improve the signal by using multiple eigenvector pairs, weighted with Gaussian profile functions of the eigenvalues, providing a basis for a generalized eigenvalue problem (GEVP), as it was recently introduced to improve distillation in meson spectroscopy. We show results with the new method for the static potential with dynamical fermions and demonstrate its efficiency compared to traditional Wilson loop calculations. The method presented here can also be applied to compute hybrid or tetra-quark potentials and to static-light systems.

The 39th International Symposium on Lattice Field Theory, LATTICE2022
August, 8-13, 2022
Bonn, Germany

*Speaker

PoS(LATTICE2022)060

1. Introduction

We have developed a code for the calculation of the static potential energy based on the method presented in [1], first proposed in [2] and also suggested in [3, 4], where the spatial Wilson lines $U_s(\vec{x},\vec{y},t)$ of a classical Wilson loop $W(R,T)$ of size $(R=|\vec{y}-\vec{x}|)\times(T=|t_1-t_0|)$ are replaced by 3D Laplacian eigenvector pairs $v(\vec{x},t)v^\dagger(\vec{y},t)$[1] corresponding to the lowest eigenvalues λ:

$$\begin{aligned} W(R,T) &= \left\langle \mathrm{Tr}[U_t(\vec{x};t_0,t_1)U_s(\vec{x},\vec{y},t_1)U_t^\dagger(\vec{y};t_0,t_1)U_s^\dagger(\vec{x},\vec{y},t_0)] \right\rangle \\ &\to \left\langle \mathrm{Tr}[U_t(\vec{x};t_0,t_1)v(\vec{x},t_1)v^\dagger(\vec{y},t_1)U_t^\dagger(\vec{y};t_0,t_1)v(\vec{y},t_0)v^\dagger(\vec{x},t_0)] \right\rangle \equiv L(R,T)\,, \quad (1) \end{aligned}$$

with $U_t(\vec{x},t_0,t_1)$ the temporal (static) Wilson line at space point $\vec{x}$ from time t_0 to t_1. Sandwiched between two eigenvectors at corresponding start- and end-times $v(\vec{x},t_0)$ and $v(\vec{x},t_1)$, it gives a static quark line $Q(\vec{x},t_0,t_1)=v^\dagger(\vec{x},t_0)U_t(\vec{x},t_0,t_1)v(\vec{x},t_1)$ at $\vec{x}$ of time extent $T=|t_1-t_0|$. Its expectation value $\langle Q(\vec{x},T)\rangle$ of course vanishes except for $T=0$. When combined with another static quark line $\bar{Q}(\vec{y},t_0,t_1)$ at $\vec{y}$, it gives the above Laplace trial state $L(R,T)$ in $Eq.$ (1) for $R=|\vec{y}-\vec{x}|$, depicted in Fig. 1.

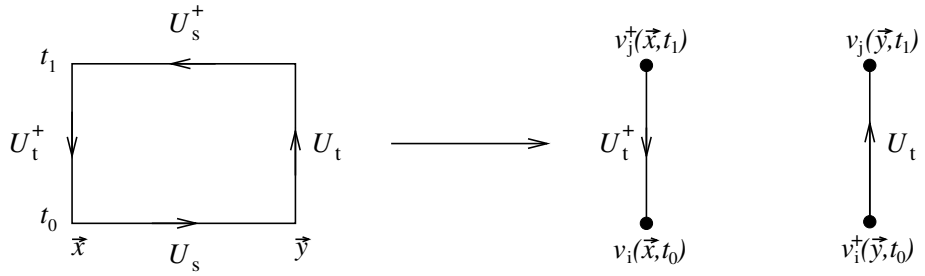

Figure 1: The spatial Wilson lines $U_s(\vec{x},\vec{y},t)$ of the classical Wilson loop $W(R,T)$ of size $(R=|\vec{y}-\vec{x}|)\times(T=|t_1-t_0|)$ (left) can be replaced by Laplacian eigenvector pairs $v^\dagger(\vec{x},t)v(\vec{y},t)$ (right).

$v(\vec{x},t)v^\dagger(\vec{y},t)$ represents all possible paths from $\vec{x}$ to $\vec{y}$ on the lattice, hence, we can not only form straight lines (on-axis), but also off-axis paths very easily, which would correspond to very complicated stair-like constructions of link variables. In fact, this simple method of measuring of off-axis spatial Wilson lines and loops is one of the main advantages of this method. Many off-axis separations are required for a fine resolution of the static potential which is important, *e.g.*, when performing a detailed investigation of string breaking [5, 6] or when matching the perturbative and the lattice QCD static potential to determine the scale $\Lambda_{\overline{\mathrm{MS}}}$ [7–11].

We present an improvement of Eq. (1) using not only the eigenvector corresponding to the lowest eigenvalue, but a number N_v of lowest eigenvectors v_i weighted with Gaussian profiles depending on their eigenvalues λ_i. A similar method was successfully applied to hadronic correlation functions in [12] where an optimal smearing profile was introduced in the distillation framework [13], which can be equivalently expressed as an optimal creation operator for a meson. In the case of the static potential we get an improvement for the static energies, which reach their plateau values at earlier temporal distances, to be quantified below.

[1]Indeed, $U_s(\vec{x},\vec{y},t)$ and $v(\vec{x},t)v^\dagger(\vec{y},t)$ have the same gauge transformation behavior.

2. The improved static energy based on Laplacian eigenvectors

First, we write the classical Wilson loop of size $(R = |\vec{x} - \vec{y}|) \times (T = |t_1 - t_0|)$ using trial states which are formed by eigenvector components of the covariant lattice Laplace operator as a transfer matrix[2] of $N_v \times N_v$ eigenvectors v_i and v_j in time slices t_0 and t_1 respectively,

$$L_{ij}(R,T) \quad = \quad \sum_{\vec{x},t_0} \left\langle \mathrm{Tr}[v_i^\dagger(\vec{x},t_0) U_t(\vec{x};t_0,t_1) v_j(\vec{x},t_1) v_j^\dagger(\vec{y},t_1) U_t^\dagger(\vec{y};t_0,t_1) v_i(\vec{y},t_0)] \right\rangle. \qquad (2)$$

We could either take a double sum over all eigenvector pairs $i, j = 1 \ldots N_v$, which increases the statistics and the signal of the Wilson loops or we can solve a GEVP for the Laplacian state basis matrix L_{ij}, which however is very ill-conditioned. We therefore prune L_{ij} using the three most significant singular vectors u_k from a singular value decomposition[3] via $\tilde{L}_{kl} = u^\dagger_{k,i} L_{ij} u_{l,j}$, which keeps only (a combination) of useful operators and improves the stability of the GEVP for fixed R/a: $\tilde{L}(t) v_k(t,t_0) = \mu_k(t,t_0) \tilde{L}(t_0) v_k(t,t_0)$. From the principal correlators $\mu_k(t,t_0)$ we get the effective energies/masses. From the vectors $v_k(t,t_0)$ and u_k we see that the GEVP favors low-lying eigenmodes. On the other hand, an increasing number N_v of eigenvectors enhances the signal and in particular the overlap with the ground-state in the effective energies/masses for small distances.

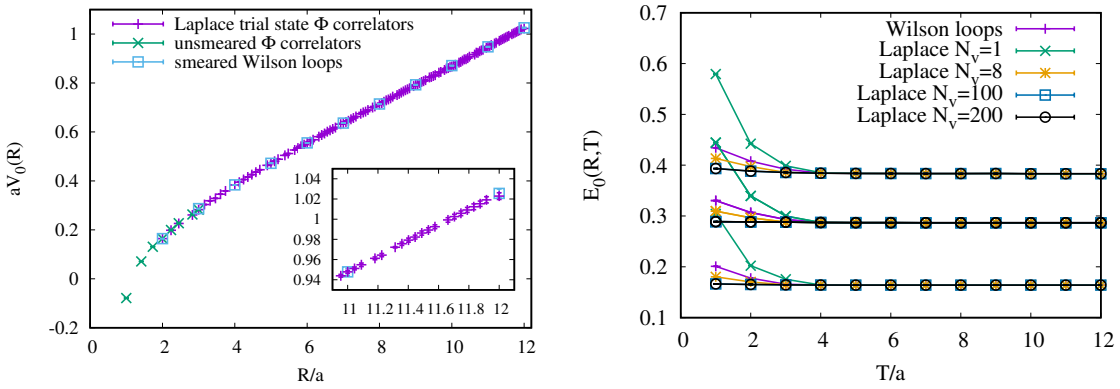

Figure 2: The static potential (left) and three effective energies/masses (right) on ensemble Em1 using the Laplacian eigenvector approach. The first is computed for all (!) on- **and off**-axis separations R/a, compared to on-axis Wilson loops. The green points for $R/a \leq 3$ result from un-smeared Laplace trial state correlators (no HYP), showing the Coulomb behavior of the potential at small R, these are shifted vertically to match the potential with HYP2 smeared temporal links at $R/a = 2$. The ground state overlap can be drastically improved by using more eigenvectors, see Table 1, we get earlier plateaus for larger N_v.

In Fig. 2 we show our results for the new observable compared to actual Wilson loop measurements on a $24^3 \times 48$ lattice ensemble at $\beta = 5.3$ ($a = 0.0658$fm) and $N_f = 2$ non-perturbatively $O(a)$-improved Wilson quarks with $\kappa = 0.13270$, corresponding to half the charm quark mass. The original Wilson loop was measured on 4646 gauge configurations, while L_{ij} was measured

[2]We thank Jeff Greensite for a fruitful discussion which lead to this slightly different approach compared to the analysis presented in the original talk.

[3]$L_{ij} = UDV^\dagger$ with U and V being unitary matrices, whose column vectors u_k and v_l form an orthonormal basis, and D being diagonal with non-negative real numbers on the diagonal.

on every fourth configuration only (1160 measurements). In the left plot we present the static potential $aV_0(R) = \lim_{T\to\infty} \log[L(R,T)/L(R,T+a)]$ for all on- and off-axis separations R/a from Laplacian eigenvector pairs compared to on-axis Wilson loop results. In the measurement of Wilson loops all gauge links are HYP2 smeared [14]. We want to note that contrary to Wilson loops, Laplace trial states have an exact symmetry of the potential around half the lattice extension (in a specific direction $\vec{r}$), where in fact the force between $Q\bar{Q}$ must vanish due to the periodic boundary conditions, *i.e.*, the static potential should be flat. The right plot in Fig. 2 clearly shows that an increasing number N_v of Laplacian eigenvector pairs improves the ground state overlap of the effective energies/masses for the static quark-anti-quark system. Already $N_v = 8$ eigenvector pairs reach the plateau values faster than the original Wilson loops, while at $N_v = 100$ the effect seems to saturate, we do not see a difference between $N_v = 100$ and $N_v = 200$. The ground state overlaps can be quantified by taking the t-average over the mass-plateau region of

$$\frac{L(R,t)}{L(R,t_0)} \frac{\cosh\left(\left(\frac{T}{2}-t_0\right) aV_0(R)\right)}{\cosh\left(\left(\frac{T}{2}-t\right) aV_0(R)\right)}, \tag{3}$$

using the same $t_0 = 3$ as in the GEVP and corresponding ground state energiesd $aV_0(R)$ from a cosh-fit. These so-called 'fractional overlaps' are listed in Table 1 and underpin again, that a large number N_v of eigenvector pairs gives better overlaps for small distances R/a, but with decreasing importance especially for large distances, where already $N_v < 100$ shows better overlaps.

R/a	$N_v = 1$	8	64	100	200	Gauss	Wloop	GEVP
1	0.773(3)	0.945(1)	0.970(1)	0.980(1)	0.982(1)	0.993(1)	0.921(1)	0.983(1)
2	0.747(4)	0.929(2)	0.964(1)	0.988(1)	0.987(1)	0.989(1)	0.891(1)	0.978(1)
3	0.723(4)	0.878(2)	0.984(2)	0.987(2)	0.986(1)	0.988(1)	0.867(1)	0.972(2)
4	0.726(5)	0.874(3)	0.921(2)	0.982(2)	0.984(2)	0.986(2)	0.841(2)	0.965(3)
5	0.637(6)	0.871(4)	0.979(3)	0.983(3)	0.982(3)	0.983(3)	0.813(2)	0.956(5)
6	0.629(6)	0.869(4)	0.978(4)	0.981(4)	0.980(3)	0.981(3)	0.793(3)	0.948(6)
7	0.619(7)	0.869(5)	0.977(4)	0.982(4)	0.979(4)	0.987(4)	0.772(3)	0.934(7)
8	0.598(8)	0.862(6)	0.972(5)	0.971(5)	0.970(4)	0.974(4)	0.745(4)	0.953(8)
9	0.572(8)	0.857(6)	0.960(5)	0.954(5)	0.934(4)	0.963(3)	0.708(4)	0.947(9)
10	0.540(9)	0.840(7)	0.955(5)	0.941(6)	0.931(5)	0.965(1)	0.671(5)	0.94(1)
11	0.426(9)	0.807(7)	0.943(6)	0.934(5)	0.93(1)	0.956(9)	0.649(4)	0.93(1)
12	0.33(7)	0.79(2)	0.94(1)	0.932(9)	0.92(1)	0.95(1)	0.64(2)	0.92(1)

Table 1: Fractional overlaps with the corresponding ground state energies $aV_0(R)$. In general, an increasing number N_v of Laplacian eigenvectors enhances the overlap up to about $N_v \approx 100$ and are already better for $N_v = 8$ than standard Wilson loops (column 7). The overlaps for Laplace trial states from a GEVP with Gaussian profiles in the 6th column are better than Wilson loop results from a GEVP with different spatial HYP smearing levels (column 8), see text below.

Therefore, instead of feeding a large ill-conditioned $N_v \times N_v$ transfer matrix to the GEVP we introduce Gaussian profile functions $\exp(-\lambda^2/2\sigma^2)$ for each eigenvector with the corresponding

eigenvalue λ and different Gaussian widths σ. We define the new GEVP basis matrix

$$\mathcal{L}_{kl}(R,T) \quad = \quad \sum_{i,j}^{N_v} N_{kl}(\lambda_i,\lambda_j) L_{ij}(R,T), \tag{4}$$

by (double-)summing over the N_v eigenvector pairs[4], weighted by Gaussian profile functions

$$N_{kl}(\lambda_i,\lambda_j) = \exp(-\lambda_i^2/2\sigma_k^2)\exp(-\lambda_j^2/2\sigma_l^2)$$

with $\sigma_{k,l} \in [0.05, 0.0894, 0.1289, 0.1683, 0.2078, 0.2472, 0.2867]$, see Fig. 3 (left). This way we gain statistics (precision) by the double sum and find an optimal number of 'important' eigenvectors by solving the GEVP for the Wilson loop basis matrix $\mathcal{L}_{kl}$ using combinations of profiles with different $\sigma_{k,l}$. Again, we first prune $\mathcal{L}_{kl}$ using the three most significant singular vectors u_m via $\tilde{\mathcal{L}}_{mn} = u^\dagger_{m,k}\mathcal{L}_{kl}u_{n,l}$, which keeps only (a combination) of useful operators and improves the stability of the GEVP for fixed R/a: $\tilde{\mathcal{L}}(t)v^{(n)}(t,t_G) = \mu^{(n)}(t,t_G)\tilde{\mathcal{L}}(t_G)v^{(n)}(t,t_G)$.. From the principal correlators $\mu_i(t,t_0)$ we get the effective energies/masses. From the generalized eigenvectors $v^{(n)}$ and singular vectors u_i we get the 'optimal' profiles $\rho_R^{(n)} = \sum_{k,l} v_k^{(n)} u_{k,l} e^{-\lambda_i^2/2\sigma_l^2}$, depicted in blue, red and green in Fig. 3 (right) for $R/a = 4$. Indeed, the 'optimal' profiles give us a number $N_v \approx 100$ of 'important' eigenvectors for $R/a = 4$, for larger R this number slightly decreases.

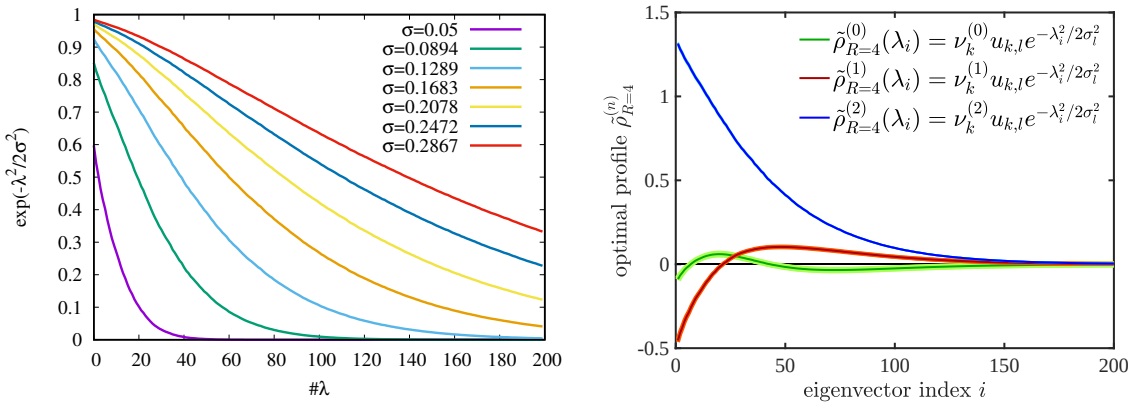

Figure 3: The Gaussian profiles (left) pruned by SVD vectors to 'optimal' profiles (right) for the GEVP.

3. Results of the improved static energy computation

With the method presented in the previous section, the implementation of [1], see also Eq. (1), using only the eigenvector corresponding to the lowest eigenvalue, can be significantly improved by (double-)summing over the lowest N_v eigenvector pairs, weighted by Gaussian profile functions using their corresponding eigenvalues $\exp(-\lambda^2/2\sigma^2)$ and different Gaussian widths $\sigma_{k/l}$. Just like for the standard Wilson loop, where we solve a generalized eigenvalue problem for the correlation matrix of Wilson loops with different spatial smearing levels, we feed $\mathcal{L}_{kl}$ from Eq. (4) (or its

[4]Actually, the sum over t_0 in Eq. (2) should be the outer most in Eq. (4), since the eigenvalues minimally vary between time-slices, however using the average eigenvalues over all time-slices does not change the final results or precision.

pruned version) into a GEVP which gives us the 'optimal' profiles or most important eigenvector pairs for each R/a. We present the improvement of effective energies using our method in the left plot of Fig. 4, showing the effective energies/masses using the improved Laplacian eigenvector approach with Gaussian profiles after solving the GEVP together with smeared Wilson loop results. In fact, the results from Laplacian modes show higher accuracy than those from Wilson loops, even though measured only on a fourth of the total statistics, however we increased the averaging by the double-sum over different eigenvectors.

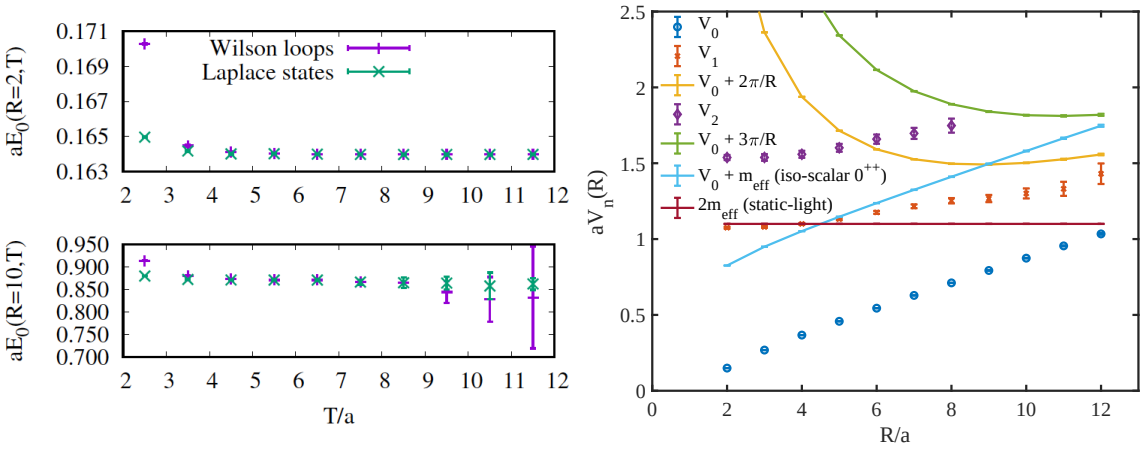

Figure 4: The effective energies/masses (left) using the Laplacian eigenvector approach with Gaussian profiles and Wilson loops with spatial HYP smearing after solving the GEVP, and static potentials V_n (right) for the ground ($n = 0$) and excited ($n = 1, 2$) states, which we compare with the excited string states $V_0+(n+1)\pi/aR$, the lowest 0^{++} iso-scalar meson (possible glueball) state $V_0+am_{\rm eff}$(iso-scalar 0^{++}) from [15] and two times the static-charm meson mass, which was also evaluated using the new method.

The right plot of Fig. 4 presents the static potentials V_n for the ground ($n = 0$) and first excited ($n = 1$) states using the Laplacian eigenvector approach with Gaussian profiles after solving the GEVP. The excited states ($n = 1, 2$) are just included to show the potential of the method.

4. Computational advantage and timings

The computational effort of this new method is even favorable to the standard Wilson loop calculation, especially for off-axis separations. In fact, for our test ensemble on a $24^3 \times 48$ lattice the computation of on-axis Wilson loops using 4 spatial smearing levels (0, 10, 20, 30 HYP steps) [14] is equally expensive as the calculation of 100 Laplacian eigenvectors and Laplace states with 3 Gaussian profiles including off-axis distances.

The computational advantage arises from the fact that the eigenvector pairs $VV^\dagger$ in Eq. (1) can be split up due to the trace to form the static quark $Q(\vec{x}, t_0, t_1) = v^\dagger(\vec{x}, t_0)U_t(\vec{x}, t_0, t_1)v(\vec{x}, t_1)$ and anti-quark $\bar{Q}(\vec{x}, t_0, t_1) = v^\dagger(\vec{y}, t_1)U_t^\dagger(\vec{y}, t_0, t_1)v(\vec{y}, t_0)$ lines, which can be contracted separately at all $\vec{x}$ resp. $\vec{y}$ first to a complex number at each position, which then can easily be multiplied for arbitrary on- and off-axis separations without the need to compute complicated stair-like connections.

5. Conclusions & Outlook

We presented an alternative operator for a static quark-anti-quark pair based on Laplacian eigenmodes and improved the operator given in [1] using a large number of eigenvectors weighted with Gaussian profiles. We observe earlier plateaus in the effective masses and a better signal. The main advantage of this eigenvector approach however is to have an efficient method to compute the static potential not only for on-axis, but also for many off-axis quark-antiquark separations. Using the standard gauge link approach for the computation of Wilson loops, is rather time consuming, since a large number of stair-like gluonic connections has to be computed (cf. *e.g.* [5] for a discussion of how to compute such off-axis Wilson loops). In comparison, computing many off-axis separations of the static potential using Laplacian eigenvectors requires less computing time, since the eigenvector components of the covariant lattice Laplace operator have to be computed only once and can then be used for arbitrary on-axis and off-axis separations without the need to compute stair-like connections.

We want to adapt the method to also measure hybrid static potentials relevant for exotic mesons, where the gluonic string excitations (gluonic handles in the standard Wilson loop approach) can be realized by covariant derivatives of the Laplacian eigenvectors in Eq. (1). Finally, when we combine our static quark line with a perambulator from [12], we can build a static-light quark meson. The long-term plan is to put together all building blocks for observation of string breaking in QCD (mixing matrix of static and light quark propagators) in the framework of distillation [13]. For more details on the derivation of the method and possible applications please see [16].

Acknowledgements

The authors gratefully acknowledge the Gauss Centre for Supercomputing e.V. (www.gauss-centre.eu) for funding this project by providing computing time on the GCS Supercomputer SuperMUC-NG at Leibniz Supercomputing Centre (www.lrz.de). The work is supported by the German Research Foundation (DFG) research unit FOR5269 "Future methods for studying confined gluons in QCD", the Ministry for Culture and Science of the State of North Rhine-Westphalia (MKW NRW) under the funding code NW21-024-A and EU grant agreement 824093 (STRONG-2020). For valuable discussions we thank Pedro Bicudo, Jeff Greensite, Tomasz Korzec and especially Juan Andrés Urrea-Niño, who also provided the Laplacian eigenvectors used in this work.

References

[1] T. Neitzel, J. Kämper, O. Philipsen, and M. Wagner, "Computing the static potential using non-string-like trial states," *PoS* **LATTICE2016** (2016) 112, arXiv:1610.05147 [hep-lat].

[2] P. de Forcrand and O. Philipsen, "Adjoint string breaking in 4-D SU(2) Yang-Mills theory," *Phys. Lett. B* **475** (2000) 280–288, arXiv:hep-lat/9912050.

[3] O. Philipsen, "Nonperturbative formulation of the static color octet potential," *Phys. Lett. B* **535** (2002) 138–144, arXiv:hep-lat/0203018.

[4] O. Jahn and O. Philipsen, "The Polyakov loop and its relation to static quark potentials and free energies," *Phys. Rev. D* **70** (2004) 074504, arXiv:hep-lat/0407042.

[5] **SESAM** Collaboration, G. S. Bali, H. Neff, T. Duessel, T. Lippert, and K. Schilling, "Observation of string breaking in QCD," *Phys. Rev. D* **71** (2005) 114513, arXiv:hep-lat/0505012.

[6] J. Bulava, B. Hörz, F. Knechtli, V. Koch, G. Moir, C. Morningstar, and M. Peardon, "String breaking by light and strange quarks in QCD," *Phys. Lett. B* **793** (2019) 493–498, arXiv:1902.04006 [hep-lat].

[7] N. Brambilla, X. Garcia i Tormo, J. Soto, and A. Vairo, "Precision determination of $r_0\Lambda^{-}_{MS}$ from the QCD static energy," *Phys. Rev. Lett.* **105** (2010) 212001, arXiv:1006.2066 [hep-ph]. [Erratum: Phys.Rev.Lett. 108, 269903 (2012)].

[8] **ETM** Collaboration, K. Jansen, F. Karbstein, A. Nagy, and M. Wagner, "$\Lambda_{\bar{MS}}$ from the static potential for QCD with $n_f = 2$ dynamical quark flavors," *JHEP* **01** (2012) 025, arXiv:1110.6859 [hep-ph].

[9] A. Bazavov, N. Brambilla, X. Garcia i Tormo, P. Petreczky, J. Soto, and A. Vairo, "Determination of α_s from the QCD static energy," *Phys. Rev. D* **86** (2012) 114031, arXiv:1205.6155 [hep-ph].

[10] A. Bazavov, N. Brambilla, X. G. Tormo, I, P. Petreczky, J. Soto, and A. Vairo, "Determination of α_s from the QCD static energy: An update," *Phys. Rev. D* **90** no. 7, (2014) 074038, arXiv:1407.8437 [hep-ph]. [Erratum: Phys.Rev.D 101, 119902 (2020)].

[11] F. Karbstein, A. Peters, and M. Wagner, "$\Lambda_{\overline{\rm MS}}^{(n_f=2)}$ from a momentum space analysis of the quark-antiquark static potential," *JHEP* **09** (2014) 114, arXiv:1407.7503 [hep-ph].

[12] F. Knechtli, T. Korzec, M. Peardon, and J. A. Urrea-Niño, "Optimizing creation operators for charmonium spectroscopy on the lattice," *Phys. Rev. D* **106** no. 3, (2022) 034501, arXiv:2205.11564 [hep-lat].

[13] **Hadron Spectrum** Collaboration, M. Peardon, J. Bulava, J. Foley, C. Morningstar, J. Dudek, R. G. Edwards, B. Joo, H.-W. Lin, D. G. Richards, and K. J. Juge, "A Novel quark-field creation operator construction for hadronic physics in lattice QCD," *Phys. Rev. D* **80** (2009) 054506, arXiv:0905.2160 [hep-lat].

[14] M. Donnellan, F. Knechtli, B. Leder, and R. Sommer, "Determination of the Static Potential with Dynamical Fermions," *Nucl. Phys. B* **849** (2011) 45–63, arXiv:1012.3037 [hep-lat].

[15] J. A. Urrea-Niño, F. Knechtli, T. Korzec, and M. Peardon, "Optimized meson operators for charmonium spectroscopy and mixing with glueballs," *PoS* **LATTICE2022** (2022) 087.

[16] R. Höllwieser, F. Knechtli, T. Korzec, M. Peardon, and J. A. Urrea-Niño, "Constructing static quark-anti-quark creation operators from Laplacian eigenmodes," arXiv:2212.08485 [hep-lat].